NOAA Technical Memorandum NESS 113

SATELLITE IDENTIFICATION OF SURFACE RADIANT TEMPERATURE FIELDS OF SUBPIXEL RESOLUTION

Washington, D.C.
December 1980

U.S. DEPARTMENT OF COMMERCE

NOAA Technical Memorandum NESS 113

SATELLITE IDENTIFICATION OF SURFACE RADIANT TEMPERATURE FIELDS OF SUBPIXEL RESOLUTION

Jeff Dozier

Washington, D.C.
December 1980

[NTIS Ref: PB81-184038]

UNITED STATES
DEPARTMENT OF COMMERCE
Philip M. Klutznick, Secretary

NATIONAL OCEANIC AND
ATMOSPHERIC ADMINISTRATION
Richard A. Frank, Administrator

National Earth Satellite Service
David S. Johnson,
Assistant Administrator

Satellite Identification of Surface Radiant Temperature Fields of Subpixel Resolution

Jeff Dozier 1980

NOAA National Earth Satellite Service
Earth Sciences Laboratory
Washington, DC 20233

(on leave from University of California, Santa Barbara)

ABSTRACT. A method is presented for identifying from NOAA TIROS-N series satellite data the magnitudes and subpixel areal coverages of two different surface radiant temperatures, using the different response of the Planck function at different wavelengths.

1. Introduction

Satellite spaceborne radiometers with more than one thermal infrared channel were originally designed to identify cloud-contaminated pixels and to evaluate the radiant contribution from atmospheric water vapor. However, over a surface with markedly varying temperatures at sub-pixel resolution, the different radiant temperatures sensed at different wavelengths may be more a result of the surface temperature field than of atmospheric interference with the signal.

Over a land surface with two different surface materials of different temperatures, the way in which the radiance contributions are averaged over a pixel will depend on the wavelength range of the sensor. If one part of a pixel is much warmer than the remainder, for example, that warm part will contribute proportionally more radiance to the signal in shorter wavelengths of the thermal infrared than in longer wavelengths. Through manipulation of the integral of the Planck function for the different channels, we can calculate (a) the radiant temperatures of one of two temperature fields of sub-pixel resolution; and (b) the portions of the pixel that each occupies. The portions of a pixel occupied by each temperature field are not necessarily contiguous, but the method assumes that there are only two temperature fields, with a "target" temperature and a "background" temperature.

2. TIROS-N Satellite Series Thermal Infrared Sensors

NOAA's TIROS-N series polar orbiting satellites now contain instrumentation for measuring upwelling thermal infrared radiation in more than one wavelength band. The Advanced Very High Resolution Radiometer (AVHRR) on NOAA-6 (launched June 1979), with a spatial resolution of 1.1 km, has two thermal infrared channels. On later satellites in the series, a third thermal channel will be added to the AVHRR. Wavelength ranges for these instruments are given in table 1.

Table 1
AVHRR Thermal Channels (from Schwalb 1979)

NOAA-6

channel	wavelength range (μm)
3	3.55 - 3.93
4	10.5 - 11.5

NOAA-7 and subsequent satellites

channel	wavelength range (μm)
3	3.53 - 3.93
4	10.4 - 11.3
5	11.4 - 12.4

Channels 3 and 4 on these satellites are in water vapor window regions of the electromagnetic spectrum. The design purpose of the two channels was to allow discrimination of cloud-contaminated pixels, and to provide a radiance measurement in a highly transmissive water vapor window, for the measurement of sea surface temperature, chiefly at night. The third thermal infrared channel will add capability to determine absolute sea surface temperature day or night.

3. Notation

c_1	first Planck constant ($3.741832\times10^{-16}\ W\,m^2$)
c_2	second Planck constant ($1.438786\times10^{-2}\ m\,K$)
$L(T)$	upwelling thermal radiance ($W\,m^{-2}\,sr^{-1}$) as a function of temperature
$L_j(T)$	integrated upwelling thermal radiance in channel j ($W\,m^{-2}\,sr^{-1}$)
p	portion of a pixel occupied by target
T	temperature (K)
T_j	radiant temperature measured by channel j (K)
T_b	background temperature (K)
T_t	target temperature (K)
$\beta(\lambda,T)$	Planck function ($W\,m^{-3}$)
ϵ	emissivity
λ	wavelength (μm or m)
$\Phi(\lambda)$	relative spectral response function of sensor (normalized to 1 at maximum value)

4. Radiance-Temperature Relations

In the absence of an atmospheric contribution or attenuation, the upwelling radiance sensed by a downward pointing radiometer is derived by integrating the product of Planck's function and the response function of the sensor:

$$L(T) = \frac{1}{\pi}\int_{\lambda_1}^{\lambda_2} \epsilon_\lambda\, \beta(\lambda,T)\, \Phi(\lambda)\, d\lambda \qquad (1)$$

For most Earth surfaces ϵ_λ is nearly independent of λ over the range of an AVHRR channel, so one can drop the λ subscript and move ϵ outside the integral in (1). The Planck function

for the emittance at wavelength λ of a black body at temperature T is (Suits 1975)

$$\beta(\lambda,T) = \frac{c_1 \lambda^{-5}}{\exp\left(\frac{c_2}{\lambda T}\right) - 1}. \qquad (2)$$

The spectral response function for the sensor $\Phi(\lambda)$ is zero outside the range $[\lambda_1, \lambda_2]$. For rough calculations it is often defined as a "gate function," i.e., equal to one within the range of values specified in table 1. Alternatively, it may be defined more precisely as a graphical or tabulated function, as figure 1 shows for channels 3 and 4 of NOAA-6.

Let us designate $L_3(T)$ and $L_4(T)$ to be the NOAA-6 channel 3 and 4 radiances as functions of blackbody temperature (i.e., $\epsilon = 1$), and the inverse functions by $L_3^{-1}()$ and $L_4^{-1}()$, respectively. For temperatures from 100 to 1000 K, eq. (1) was calculated numerically by an adaptive quadrature method (Forsythe *et al.* 1977, ch. 5). The resulting values for $L_3(T)$ and $L_4(T)$ are shown in figure 2. Here it is apparent that the shift in the peak of the Planck function toward shorter wavelengths, as temperature increases, causes the radiant contribution to channel 3 to increase more rapidly, at higher temperatures, than that to channel 4.

Now, suppose we have a "mixed pixel" composed of a target at temperature T_t which occupies portion p of the pixel (where $0 \leqslant p \leqslant 1$) and a background temperature T_b which occupies the remaining portion $(1-p)$ of the pixel. The radiant temperatures sensed by the AVHRR in channels 3 and 4 will be, in the absence of an atmospheric contribution or attenuation,

$$T_j = L_j^{-1}\left[p\, L_j(T_t) + (1-p)\, L_j(T_b)\right] \quad \Big\{ j=3,4\,. \qquad (3)$$

For a reference background temperature $T_b = 285$, figure 3 shows values of T_3 and T_4 as functions of p for various values of T_t from 150 to 500 K. In figure 4 are plotted the differences $T_3 - T_4$ *vs.* p for the same situations.

5. Determination of T_t and p

Assume that we know the value of T_b, perhaps from measurements from surrounding pixels that contain no "target" surface. The two equations in (3) now have only two unknowns, p and T_t. From figure 3 it is evident that we can solve for them. For example, suppose $T_b = 285$, $T_3 = 325$, and $T_4 = 307$. The value of T_3 constrains the range of choices considerably, as shown by the dashed line in the lower graph in figure 3. The correct values for p (0.2) and T_t (371) can be selected from the value of T_4. Similarly, the correct value can be read from the difference $T_3 - T_4$ (18) in figure 4. Note that the largest differences between T_3 and T_4 occur when the pixel contains a small, hot target, or when a cold target covers almost all of the field of view. If the difference between T_t and T_b is not very large, the solution is insensitive to variations in p.

A mathematical solution that does not require the construction of graphs for every value of T_b is accomplished by rearranging eq. (3) in these simultaneous nonlinear equations:

$$L_j(T_j) - \left[p\, L_j(T_t) + (1-p)\, L_j(T_b)\right] = 0 \quad \Big\{ j=3,4\,. \qquad (4)$$

Such sets of equations can be solved by several methods. I use a modification of Brent's (1973b) algorithm developed by Moré and Cosnard (1979). Convergence problems are reduced if Box's (1966) transformation is used to map the constrained temperatures into unconstrained variables.

6. Determination of T_t when T_b and p are Unknown

For some applications, for example determination of sea surface temperature, we have no reliable estimate of the background temperature T_b. However, suppose we assume that in two adjacent pixels the target (sea surface) temperatures T_t are the same and the background (cloud) temperatures T_b are the same, but that the cloud-covered portions $(1-p)$ are different.

Note that eq. (4) can be solved for p;

$$p = \frac{L_j(T_j) - L_j(T_b)}{L_j(T_t) - L_j(T_b)} \quad \left\{ j=3,4 \right. . \tag{5}$$

If we denote the non-cloud contaminated portions of two adjacent pixels as $p^{(1)}$ and $p^{(2)}$, and their radiant temperatures by $T_j^{(1)}$ and $T_j^{(2)}$, we can form the ratio

$$\frac{p^{(1)}}{p^{(2)}} = \frac{L_j(T_j^{(1)}) - L_j(T_b)}{L_j(T_j^{(2)}) - L_j(T_b)} \quad \begin{cases} j=3,4 \\ p^{(1)} \neq p^{(2)} \neq 0 \end{cases} . \tag{6}$$

Similarly, if eq. (4) is solved for $(1-p)$ instead of p, we arrive at

$$\frac{1-p^{(1)}}{1-p^{(2)}} = \frac{L_j(T_j^{(1)}) - L_j(T_t)}{L_j(T_j^{(2)}) - L_j(T_t)} \quad \begin{cases} j=3,4 \\ p^{(1)} \neq p^{(2)} \neq 1 \end{cases} . \tag{7}$$

Although the values of the ratios in eqs. (6) and (7) are unknown, Smith and Rao (1972) have pointed out that they are independent of wavelength and therefore must be the same for all values of j. Hence

$$\frac{L_3(T_3^{(1)}) - L_3(T_x)}{L_3(T_3^{(2)}) - L_3(T_x)} - \frac{L_4(T_4^{(1)}) - L_4(T_x)}{L_4(T_4^{(2)}) - L_4(T_x)} = 0 \quad \begin{cases} T_3^{(1)} \neq T_3^{(2)} \\ T_4^{(1)} \neq T_4^{(2)} \end{cases} . \tag{8}$$

In eq. (8) the variable T_x designates some unknown temperature. Examination of the equation (see figure 5) indicates that it has two roots, T_b and T_t, and two discontinuities, $T_3^{(2)}$ and $T_4^{(2)}$. It is possible to solve (8) by an iterative method for T_b and T_t, but the method and the starting guesses must be chosen carefully. My recommendation is to use Brent's (1973a, ch. 4) algorithm. It requires two initial guesses which span the solution, but problems with the discontinuities can be avoided by ensuring that the guesses do not span either discontinuity.

Once T_b is found, it can be used in (5) to find p.

7. Corrections for Atmospheric Effects

Because some of the thermal radiation emitted by the Earth's surface is absorbed and re-emitted by the atmosphere, a radiant temperature measured from space is lower than the true surface radiant temperature. Dual thermal channels, in different wavelength bands, can be used to correct for atmospheric attenuation and thereby determine the absolute surface temperature, to within about 1 K. Prabhakara *et al.* (1974) and Morcrette and Irbe (1978) have shown theoretically that a linear correction of the following form gives the actual surface radiant temperature for a variety of possible atmospheric temperature and water vapor profiles:

$$T_{surf} - T_j = a\,(T_j - T_k) + b \tag{9}$$

T_j and T_k are satellite radiant temperature measurements in two separate channels. The coefficients a and b depend on the wavelength values of the channels. McClain and Abel (1977) have verified the method using coincident satellite and ship data sets. For channels 3 and 4 of NOAA-6 McClain (1980), using the atmospheric radiance model of Weinreb and Hill (1980), has calculated the coefficients to be $a = 0.42$ and $b = 1.3$, when $j = 3$ and $k = 4$.

To determine the necessary atmospheric correction when T_b is known, one need only determine the magnitude of the correction from the pixels surrounding the one containing the target temperature field. From these the additive correction to T_3 and T_4 can be made, and the

analysis can proceed as described in section 5.

The case where T_b and p are unknown is somewhat more complicated, but can be solved if there are three, instead of two, pixels where T_b and T_t are the same, but $p^{(1)} \neq p^{(2)} \neq p^{(3)} \neq 0$. Let us introduce the notation $T_{b,3}$ to designate the brightness temperature that the satellite would register if the entire pixel were of the background temperature, i.e., $p = 0$. Let $T_{t,3}$ designate the brightness temperature if the entire pixel were of the target temperature, i.e., $p = 1$. $T_{b,4}$ and $T_{t,4}$ are similarly defined. If we form the ratio $(1-p^{(1)})/(1-p^{(2)})$ we can derive an equation identical to (8) but with two unknowns, $T_{x,3}$ and $T_{x,4}$, instead of one. To solve for these we need an additional equation, which we form from the ratio $(1-p^{(3)})/(1-p^{(2)})$, and thereby convert eq. (8) into two simultaneous nonlinear equations.

$$\frac{L_3(T_3^{(k)}) - L_3(T_{x,3})}{L_3(T_3^{(2)}) - L_3(T_{x,3})} - \frac{L_4(T_4^{(k)}) - L_4(T_{x,4})}{L_4(T_4^{(2)}) - L_4(T_{x,4})} = 0 \quad \begin{cases} k=1,3 \\ T_3^{(1)} \neq T_3^{(2)} \neq T_3^{(3)} \\ T_4^{(1)} \neq T_4^{(2)} \neq T_4^{(3)} \end{cases} \qquad (10)$$

In eq. (10) the variables $T_{x,3}$ and $T_{x,4}$ designate the roots. There are two sets of solutions, $[T_{b,3}, T_{b,4}]$ and $[T_{t,3}, T_{t,4}]$. Once these are determined, T_b and T_t can be found from eq. (9).

8. Discussion

Under some circumstances this algorithm makes possible the determination of temperature fields of subpixel resolution. Potential applications include the following:

[1] It might be possible to determine temperatures of urban heat sources. Tests are being conducted within NOAA to estimate stack temperatures of steel plants using NOAA-6 satellite data with 1.1-km resolution.

[2] The technique might be useful in estimating surface temperatures and areal extents of geothermal areas.

[3] In areas that are partly snow covered, the method could be used to estimate the areal extent of snow in each pixel.

[4] Where there are no cloud-free pixels, but some pixels are not totally cloud-covered, the method still provides a measurement of sea-surface-temperature, including corrections for atmospheric attenuation due to water vapor.

Acknowledgements

This work was initiated and completed while I was supported by a Senior Postdoctoral Research Associateship from the National Research Council, National Academy of Sciences. I am indebted to my colleagues Michael Matson, E. Paul McClain, P. Krishna Rao, Richard Legeckis, Donald R. Wiesnet, and Larry Breaker for comments.

References

Box, M.J., (1966) A comparison of several current optimization problems, and the use of transformations in constrained problems, *Computer Journal,* 9: 67-77.

Brent, R.P., (1973a) *Algorithms for Minimization without Derivatives,* Prentice-Hall, Englewood Cliffs, NJ, 195 pp.

Brent, R.P., (1973b) Some efficient algorithms for solving systems of nonlinear equations, *SIAM Journal of Numerical Analysis,* 10: 327-344.

Forsythe, G.E., Malcolm, M.A., and Moler, C.B., (1977) *Computer Methods for Mathematical Computations,* Prentice-Hall, Englewood Cliffs, NJ, 259 pp.

Kidwell, K.B., (1979) NOAA polar orbiter data (TIROS-N and NOAA-6) users guide, NOAA Satellite Data Services Division, Washington, DC

McClain, E.P., (1980) Multiple atmospheric-window techniques for satellite-derived sea surface temperatures, *COSPAR/SCOR/IUCRM Symposium, Oceanography from Space,* Venice, Italy, May 26-30.

McClain, E.P., and Abel, P.G., (1977) Remote sensing of ocean temperature, *Conference on Satellite Applications to Marine Operations,* New Orleans, LA, November 15-17, 1977, pp. 1-9.

Morcrette, J-J., and Irbe, G.J., (1978) Atmospheric correction of remote measurements of Great Lakes surface temperature, *Proceedings, Fifth Canadian Symposium on Remote Sensing,* Victoria, B.C., August 28-31, 1978, pp. 579-586.

Moré, J.J., and Cosnard, M.Y., (1979) Numerical solution of nonlinear equations, *ACM Transactions on Mathematical Software,* 5: 64-85.

Prabhakara, C., Dalu, G., and Kunde, V.G., (1974) Estimation of sea surface temperature from remote sensing in the 11- to 13-μm window region, *Journal of Geophysical Research,* 79: 5039-5044.

Schwalb, A., (1979) The TIROS-N/NOAA A-G satellite series, NOAA Technical Memorandum NESS 95, Washington, DC, 75 pp.

Smith, W.L., and Rao, P.K., (1972) The determination of surface temperature from satellite "window" radiation measurements, *Fifth Symposium on Temperature,* Washington, DC, June 21-24, 1971, Instrument Society of America, Pittsburgh, PA, pp. 2251-2257.

Suits, G.H., (1975) The nature of electromagnetic radiation, in *Manual of Remote Sensing,* Reeves, R.G., ed., American Society of Photogrammetry, Falls Church, VA, I: 51-73.

Weinreb, M.P., and Hill, M.L., (1980) Calculation of atmospheric radiances and brightness temperatures in infrared window channels of satellite radiometers, NOAA Technical Report NESS 80, Washington, DC, 40 pp.

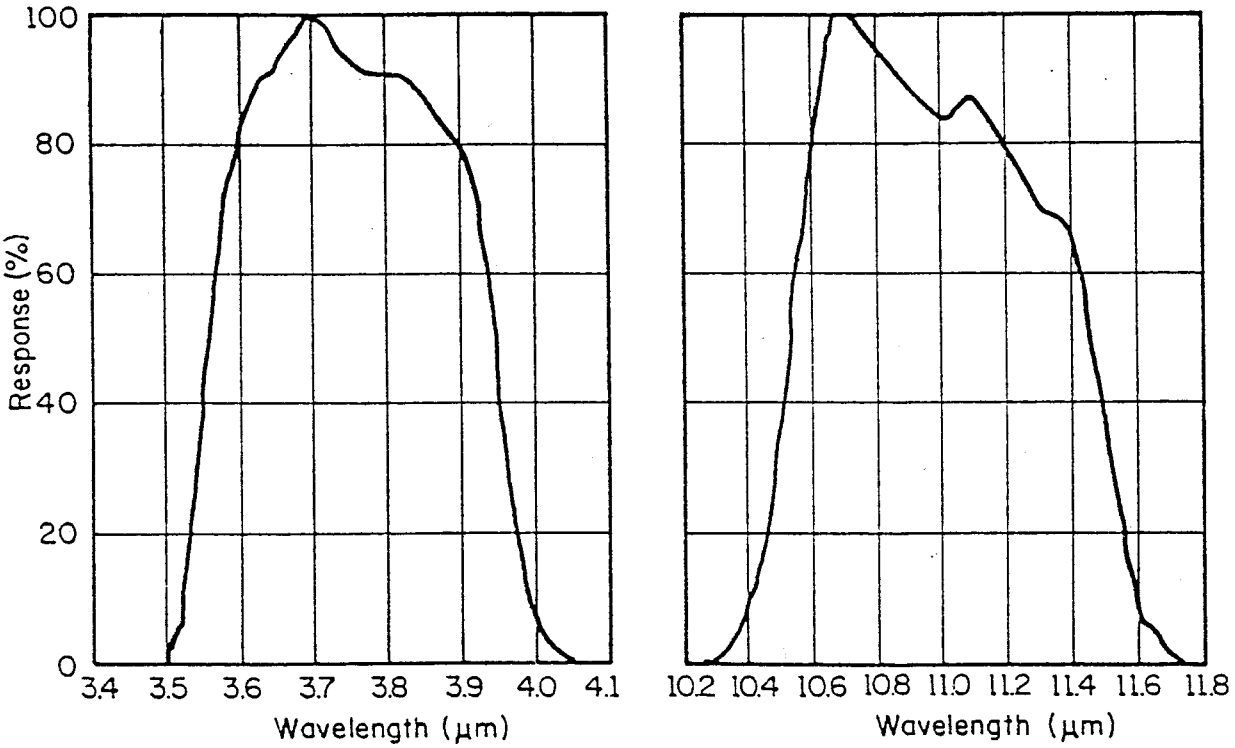

1. Relative spectral response functions (per cent) for channels 3 (left) and 4 (right) of the NOAA-6 satellite (from Kidwell, 1979).

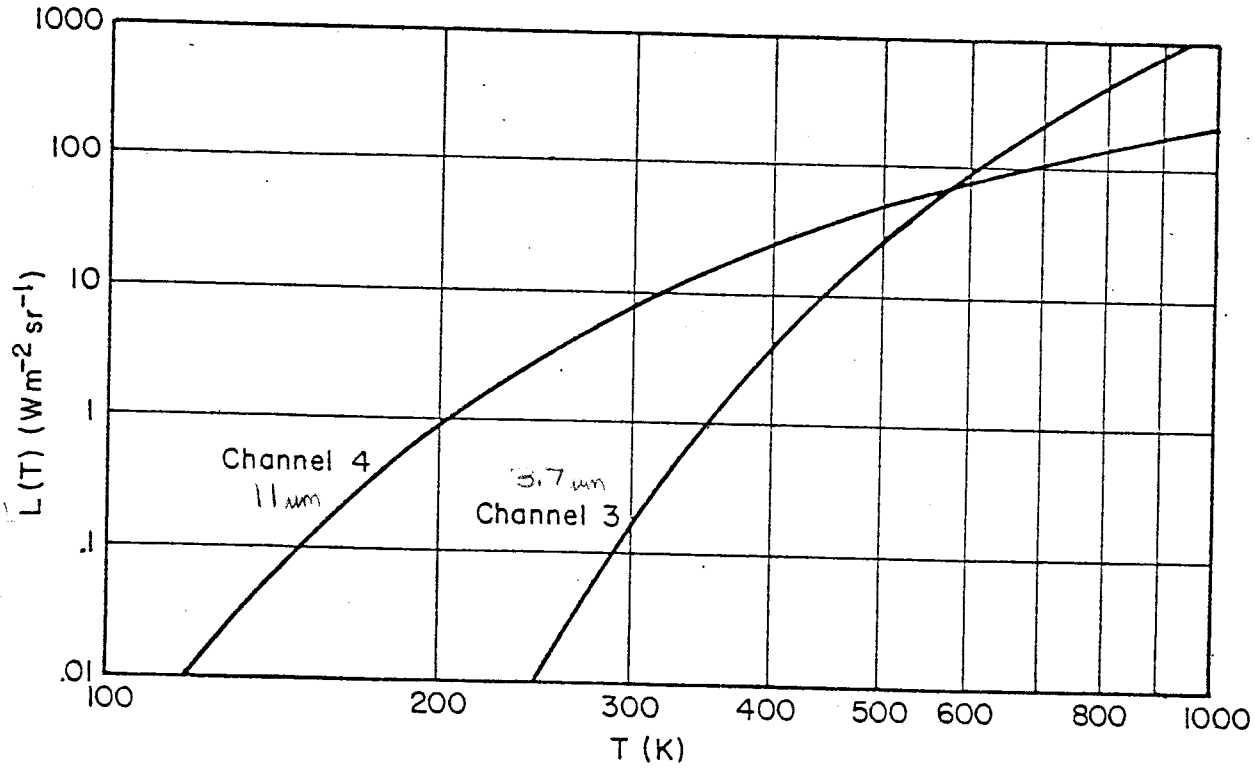

2. NOAA-6 radiances for channels 3 and 4 *vs.* temperature, as calculated by eq. (1) with the spectral response functions in figure 1.

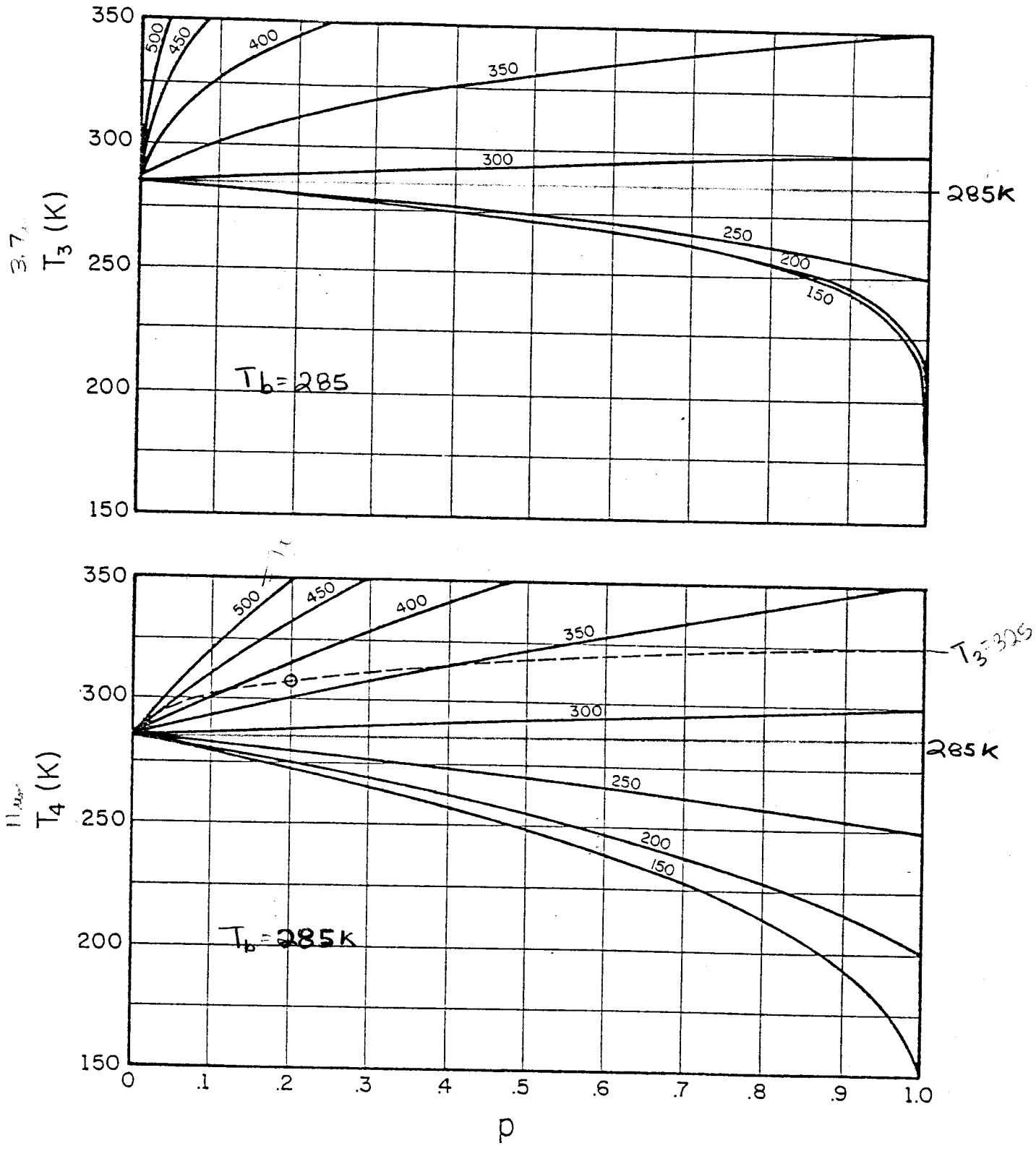

3. T_3 (top) and T_4 (bottom) *vs.* p for increasing values of T_r, for $T_b = 285$ K. The dashed line in the lower graph shows the range of values permissible when $T_3 = 325$.

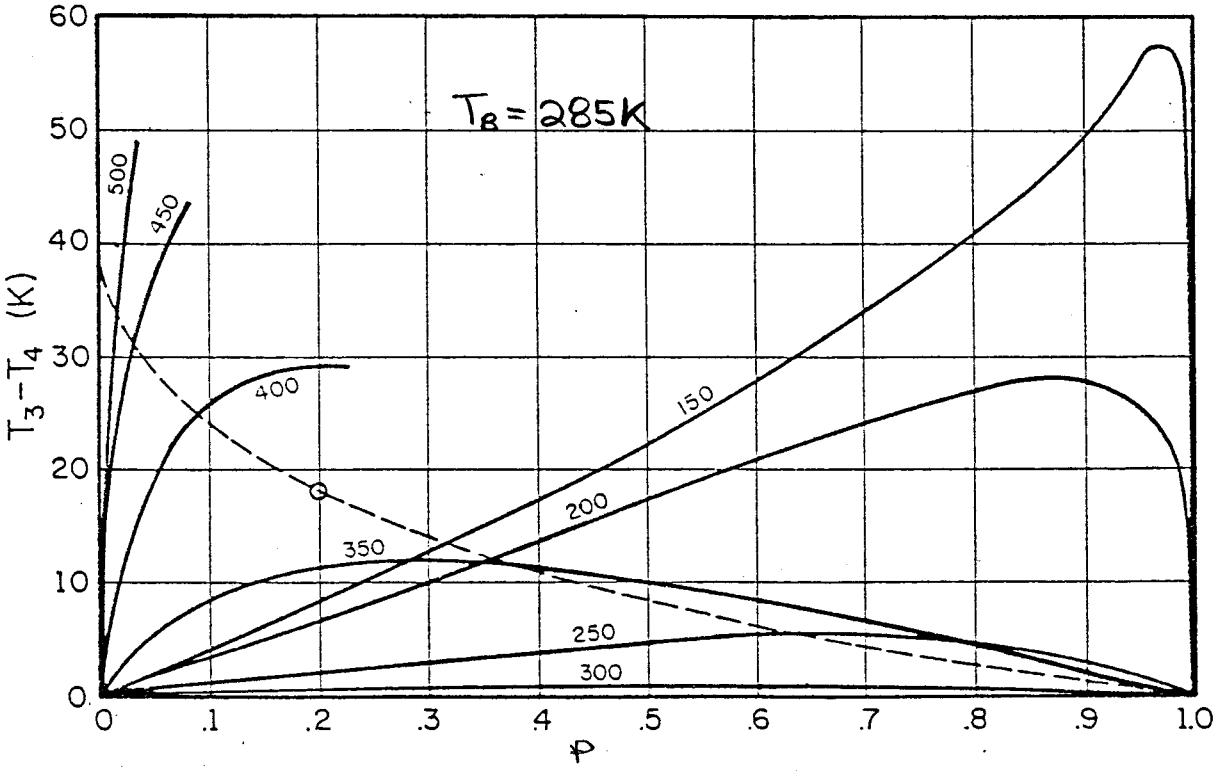

4. $T_3 - T_4$ *vs.* p for increasing values of T_t, for $T_b = 285$ K. Curves terminate where either sensor would saturate. The dashed line shows the range of values permissible when $T_3 = 325$ (but is only applicable for values of T_t which are greater than T_b).

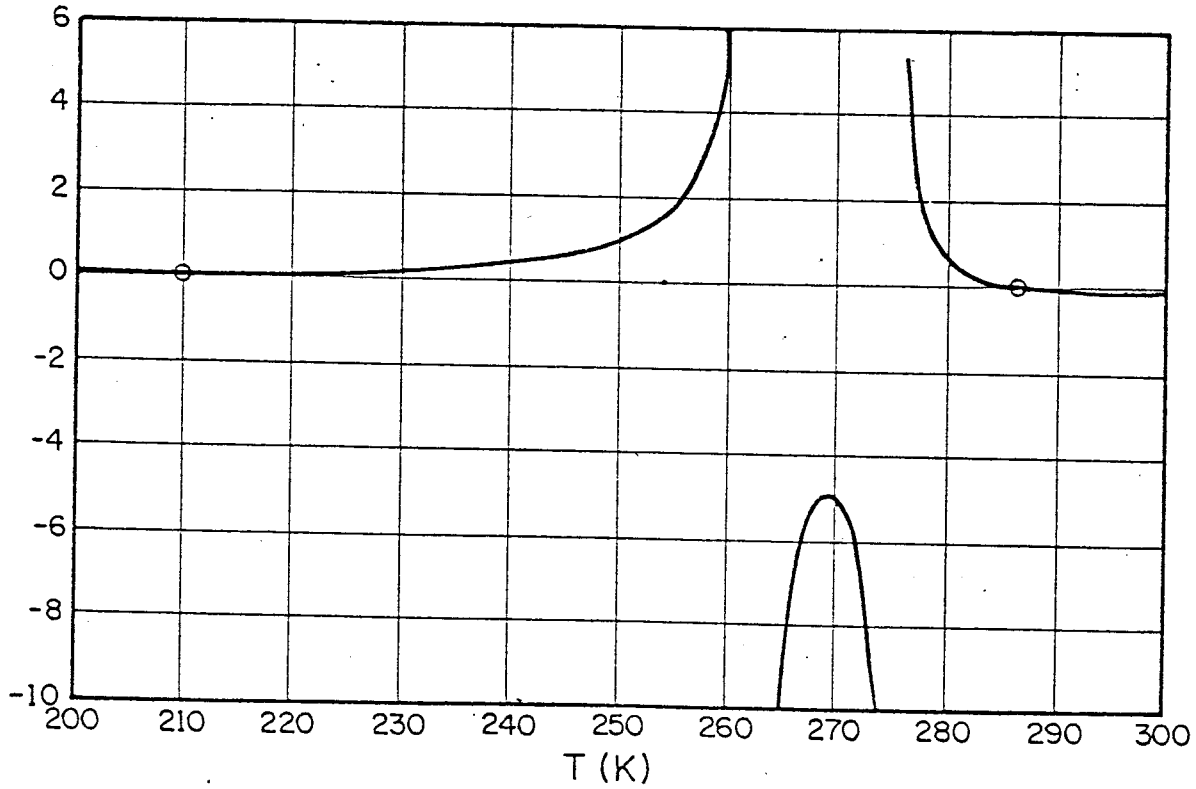

5. Graph of eq. (8) for $T_3^{(1)} = 261.4$, $T_3^{(2)} = 274.6$, $T_4^{(1)} = 241.5$, and $T_4^{(2)} = 262.9$. The solutions are $T_b = 210$ and $T_t = 285$.